Science of the Total Environment 976 (2025) 179283

Contents lists available at ScienceDirect

Science of the Total Environment

journal homepage: www.elsevier.com/locate/scitotenv

Spatial and seasonal variability of the contribution of sources to $PM_{2.5}$, PM_{10} and their oxidative potential in different sites in a central Mediterranean area

Serena Potì [a,d], Eva Merico [a], Marianna Conte [b], Florin Unga [a], Daniela Cesari [a], Adelaide Dinoi [a], Anna Rita De Bartolomeo [c], Antonio Pennetta [a], Ermelinda Bloise [a], Giuseppe Deluca [a], Giuseppe Egidio De Benedetto [e], Roberto Ferrera [f], Enrico Bompadre [f], Maria Rachele Guascito [a,c,*], Daniele Contini [a,**]

[a] Istituto di Scienze dell'Atmosfera e del Clima (ISAC), Consiglio Nazionale delle Ricerche (CNR), Lecce, Italy
[b] Istituto di Scienze dell'Atmosfera e del Clima (ISAC), Consiglio Nazionale delle Ricerche (CNR), Roma, Italy
[c] Dipartimento di Scienze e Tecnologie Biologiche ed Ambientali DiSTeBA, Università del Salento, Lecce, Italy
[d] Dipartimento di Ingegneria dell'Innovazione, Università del Salento, Lecce, Italy
[e] Dipartimento di Beni Culturali, Università del Salento, Lecce, Italy
[f] FAI Instruments s.r.l., Roma, Italy

HIGHLIGHTS

- $PM_{2.5}$, PM_{10} and their composition and oxidative potential (OP) were investigated at 22 sites.
- Spatial variability was lower than seasonal variability with the exclusion of biomass burning.
- On average, traffic and biomass burning were the major contributors to OP.
- Water insoluble OC was related to traffic while water soluble OC to biomass burning.
- Water insoluble Ca was useful to highlight the contributions of construction works.

GRAPHICAL ABSTRACT

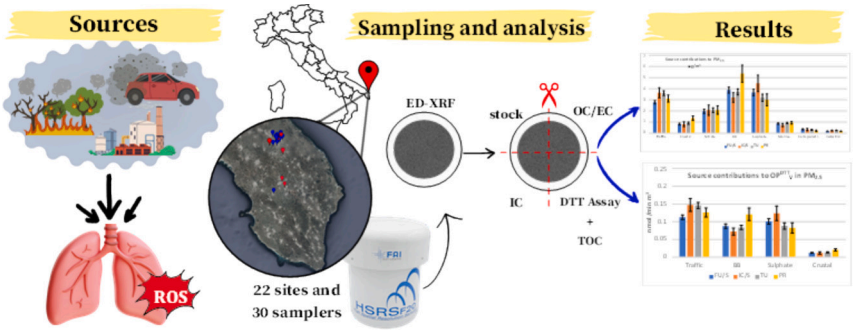

ARTICLE INFO

Editor: Pavlos Kassomenos

Keywords:
Particulate matter
Oxidative potential
Source apportionment
Spatial variability
Smart samplers

ABSTRACT

Oxidative potential (OP) is a potential indicator of negative health effects of particulate matter (PM). To address mitigation strategies, there is need of understanding how natural and anthropogenic sources influence OP at different sites. This work investigates spatial and seasonal variabilities of $PM_{2.5}$ and PM_{10} concentrations, composition, and oxidative potential (OP_V^{DTT}, obtained with DTT assay), simultaneously at 22 sites in a central Mediterranean area in south Italy. Source apportionment using PMF5 allowed to evaluate the contributions of eight sources: traffic, biomass burning (BB), nitrate, sulphate-rich, marine, crustal, carbonates/construction, and industrial (only for $PM_{2.5}$). Nitrate, traffic, and BB had larger contributions during the cold season and presented

* Correspondence to: M. R. Guascito, Dipartimento di Scienze e Tecnologie Biologiche ed Ambientali DiSTeBA, Università del Salento, Lecce, Italy.
** Correspondence to: D. Contini, Istituto di Scienze dell'Atmosfera e del Clima (ISAC), Consiglio Nazionale delle Ricerche (CNR), Lecce, Italy.
E-mail addresses: maria.rachele.guascito@unisalento.it (M.R. Guascito), d.contini@isac.cnr.it (D. Contini).

https://doi.org/10.1016/j.scitotenv.2025.179283
Received 10 January 2025; Received in revised form 9 March 2025; Accepted 27 March 2025

spatial variability with exclusion of nitrate. Industrial contributions did not have relevant seasonal or spatial variability. The other sources had an opposite trend with larger values during the warm season but only sulphate-rich had non-negligible spatial variability. OP_V^{DTT} had relevant spatial variability only during the cold season. Four sources had statistically significant contributions to OP_V^{DTT}: traffic, BB, sulphate-rich, and crustal (in descending order). The use of soluble and insoluble fractions of OC and Ca in PMF5 allowed a better separation between traffic and BB sources and allowed to determine the role of local construction works. The results may have implications in future policies for mitigation strategies of OP targeting specific sources categories.

1. Introduction

Several studies showed that exposure to atmospheric particulate matter (PM) leads to adverse health effects and the definition and implementation of mitigation strategies are societal challenges for policymakers (Basagaña et al., 2015; Ostro et al., 2016; Rivas et al., 2021). PM is a complex mixture of components with significant seasonal and spatial variability in its chemical and physical properties (Amato et al., 2016; Pietrodangelo et al., 2024) leading to relevant variability of the risk factors for human health. The variability of PM composition and physical properties is related to site-dependent physical system, e.g. activity of specific local sources, short- and long-range transport, mixing efficiency in the boundary-layer, intensity and frequency of gas-to-particle conversion processes (i.e. nucleation process), seasonal frequency of advection events (Belis et al., 2015). The toxicity of PM is related to its chemical and physical properties even if the effective mechanisms of toxicity are not fully known (Kelly et al., 2012; Rönkkö et al., 2021). The oxidative potential (OP) of particulate matter is defined as the ability of PM to catalyse, when inhaled, the formation of reactive oxygen species (ROS) leading to oxidative stress at cellular level. For this reason, in recent years, OP has emerged as a potential global indicator of health-related effects (Bates et al., 2019; Molina et al., 2020). While the correlation between oxidative potential and in vitro or in vivo biological outcomes is still uncertain (Guascito et al., 2023; Jiang et al., 2019; Lionetto et al., 2021; Øvrevik, 2019), several research efforts are currently devoted to the investigation of OP and to understand what sources are the main contributors to OP. A standard protocol and method to determine OP is not yet available (Dominutti et al., 2025). There are several acellular (i.e. chemical) approaches to determine OP: the DTT (Dithiothreitol) assay; the ascorbic acid (AA) assay, the 2,7-dichlorofluorescein (DCFH), the Ferric-Xylenol Orange (FOX) assay, and the direct ROS-quantification through OH (Dominutti et al., 2023). Each assay is sensitive to different PM components and is thereby influenced by different sources. The DTT assay is currently the most widely used approach for determination of OP. Even if epidemiological studies are usually based on PM concentrations, a recent study in Europe (Daellenbach et al., 2020) showed that the contributions of sources to PM_{10} concentration and to its OP^{DTT} are significantly different. This suggest that the information contained in spatial variability of PM and OP are effectively complementary and that it would be useful to implement reduction strategies aimed to specific sources of OP rather than to the total PM mass concentration.

Few studies have investigated the source apportionment of OP at multiple sites. The analysis of Grange et al. (2022) in different sites in Switzerland showed that combination of a metal and a wood-burning-specific tracer led to the best-performing linear models to explain OP. Moreover, anthropogenic and local road traffic and biomass burning emissions were the major contributors to OP. A study of sources impacting OP of PM_{10} based on 15-year time series at 14 different sites in France (Weber et al., 2021) showed that primary road traffic, biomass burning, dust, MSA-rich, and primary biogenic sources had distinct redox activity towards the DTT assay. In addition, site-specific sources might have an important intrinsic OP (i.e. normalised in mass) and can account for a non-negligible part of the observed OP (especially in harbour towns or near industrial plants). The study of in't Veld et al. (2023) in two sites in the Barcelona area in Spain (i.e. a rural and an urban background site) showed significantly different OP values with larger values at the urban background. OP levels were driven by anthropogenic sources: the OC-rich source, combustion, heavy oil, and road dust. Guascito et al. (2023) showed that biomass burning and traffic were the main reason of spatial variability of OP^{DTT} of PM_{10} at three sites in south Italy. An investigation of OP of PM10 at 12 sites in central Italy (18 months duration) showed that biomass burning predominated in winter, while soil dust prevailed in summer. Spatial variability in source contributions was observed due to diverse biomass types, domestic heating, and proximity to a cement plant and transportation networks (Massimi et al., 2024).

There are evidences that sources and processes impacting OP of the fine ($PM_{2.5}$) and coarse ($PM_{10-2.5}$) fractions are different (Giannossa et al., 2022; Grange et al., 2022; Paraskevopoulou et al., 2019); however, in Europe, the source apportionment studies of OP in the fine fraction are limited and even more limited are the studies including source apportionment of OP in the two size fractions. To partially fill these gaps in current research, this study was designed and focused on the characterisation of natural and anthropogenic sources at multiple sites in a central Mediterranean area in south Italy. Thirty low-volume samplers were simultaneously deployed at twenty-two sites of different typology for one year to collect $PM_{2.5}$ and PM_{10} samples. Detailed chemical analysis, and OP determination with DTT assay was done. The PMF5 (Positive Matrix Factorization) receptor model was used for source apportionment. This study aims to: (i) characterise chemical composition of $PM_{2.5}$ and PM_{10} at multiple sites in a central Mediterranean area; (ii) determine the oxidative potential of both size fractions at the different sites; (iii) identify the major sources contributing to PM and OP using a receptor modelling approach. To the best of our knowledge this is the first work addressing the seasonal and spatial variability of PM at multiple sites in this area.

2. Material and methods

2.1. Measurement instruments and sampling strategy

The instruments used to sample PM_{10} or $PM_{2.5}$ were 30 innovative smart devices (HSRS F20 - High Spatial Resolution Sampler; Fai Instruments), with a low flow rate (2 L/min), working in parallel at different sites. This kind of samplers have been specifically designed to allow spatially-resolved characterisation of PM and they can be employed to build wide and dense monitoring networks in specific areas. Monthly samples of PM_{10} and $PM_{2.5}$ were collected on quartz fibre filters (Whatman, 47 mm in diameter) thermally treated (700 °C for 2 h) to limit their initial contamination. A previous version of these samplers, with the main difference being the lower sampling flow rate (0.5 L/min across filters 37 mm in diameter), was tested and used, limited to PM_{10} at monthly time-resolution, in other research works (Massimi et al., 2020, 2021). Samplers were located in 22 different sites in the urban and suburban area of Lecce and its province territory (Fig. 1). Two samplers (i.e. one for $PM_{2.5}$ and one for PM_{10}) were collocated at 8 of these sites. HSRS sensors were installed between 9 and 20 m above ground level on the roof of public buildings, schools and private houses. The sampling campaign lasted more than one year, from December 2021 to December 2022 included. The strategy was specifically designed to investigate simultaneously spatial and seasonal variabilities of 2 PM size fractions.

2.2. Sampling sites

The study was conducted in south Italy, in the area of Lecce town (19 sites) and in its surrounding territory (3 sites). Details of the sites, including coordinates, are given in Table S1. Lecce has a population of approximately 95,700 inhabitants and it is located in the Salento peninsula. This area is influenced by local anthropogenic sources; secondary and photochemical pollution; sporadic medium range transport of pollution from industrial settlements located between 45 and 80 km in the NNW-NW direction; long range transport of Saharan dust (Conte et al., 2020).

The three sites in the province (S15, S16, and S17) were chosen because they are small villages located in a cluster with higher incidence of cancer diseases compared to the average of the region, according to the environmental authorities. In addition, one of these sites (S17), was investigated for a shorter period in a previous study and showed larger levels of organics in collected PM_{10} (Guascito et al., 2023). These sites are indicated in the following as PR. The site S1 was collocated with the Environmental-Climate Observatory (ECO) of Lecce, regional station of the Global Atmosphere Watch (GAW-WMO programme) and part of the ACTRIS network (Dinoi et al., 2023). This allowed the comparison of collected samples with results of reference instruments. The other sampling sites were chosen to represent different typologies: urban background/suburban (indicated as FU/S); urban traffic (indicated as TU); industrial/commercial centres located in suburban areas (indicated as I/CS). There are only two industrial areas with large commercial centres, one at the northern outskirt of the town and one at the southern outskirt so that both have been included in the study. The FU/S and TU sites were randomly distributed to cover the different quarters of the town. The TU sites were chosen considering the statistics of road vehicles (Conte and Contini, 2019).

2.3. Determination of $PM_{2.5}$, PM_{10}, and chemical composition

$PM_{2.5}$ and PM_{10} concentrations were determined with the reference gravimetric method (UNI EN 12341:2014). All samples were conditioned (for 48 h) in a climatised room and weighted with a microbalance (Sartorious Cubis, model MSA6.6S, ±1 μg) before and after sampling. Final concentrations were calculated by subtracting values found on field blank filters (three for each monthly dataset). Uncertainty, calculated considering the standard deviation of blanks and the expected error on sampled volumes (Conte et al., 2020) was, on average, 3.2 %.

After gravimetric determination, non-destructive ED-XRF analysis was performed to determinate the concentration of main elements of $PM_{2.5}$ and PM_{10} samples using a Spectro (XEPOS05) instrument. Measurements were performed in different phases (i.e. in both air and He atmospheres), with spinning samples, using the manufacturer "filter" protocol built in the XRF Analyser Pro software. The samples were analysed without any preparation using specifically-designed filter holders. The instrument was calibrated using 23 medium concentration elemental thin film standards from Micromatter. Specific correction factors for determination of elements on these quartz substrates was applied as determined and fully described in a previous work (Dinoi et al., 2024). The quantified elements were: Al, Ca, Cr, Cu, Fe, Mg, Mn, Na, Cl, K, Pb, Sr, Ti, Br, Rb, and Zn. Concentrations were evaluated with blank subtraction and the final typical estimated uncertainties, by means of repeatability tests and intercomparison with other laboratories were: 5 % (K, Ca, and Ti); 10 % (Na, Mg, Al, Cl, Fe, Cu, Zn, Br, Sr), and 20 % (Mn and Rb).

Successively, each filter was cut into four quarters: three quarters were used to perform chemical analysis and one quarter was saved and used, when needed, for repeatability tests. One quarter of the filter was used to obtain a punch (1 cm^2) to measure the concentrations of organic

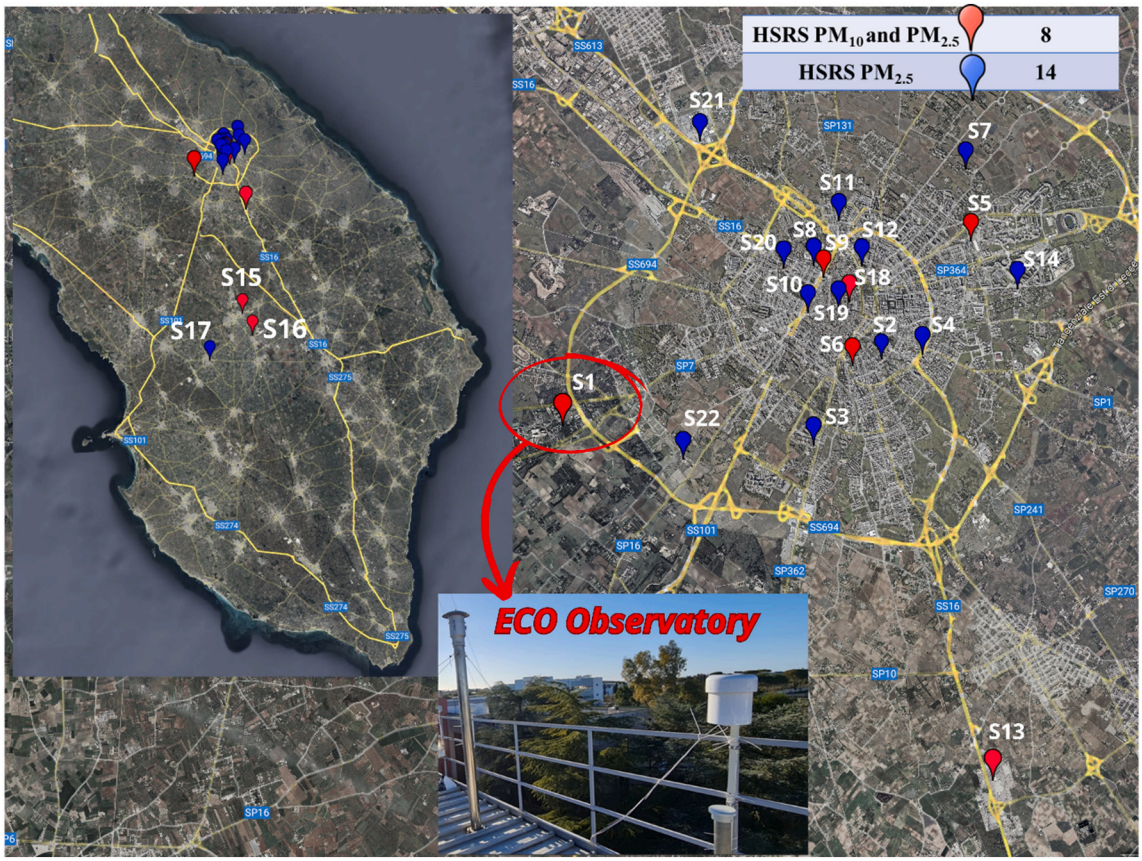

Fig. 1. Map showing location and ID of the different sites chosen for the collection of samples. Site S1 was collocated with the Environmental-Climate Observatory of Lecce.

carbon (OC) and elemental carbon (EC), using the thermo-optical analysis (Sunset OC/EC Analyser). This was operated with the EUSAAR2 protocol (Cavalli et al., 2010). An external sucrose standard solution was used for the multipoint calibration of the instrument (Merico et al., 2019). The OC and EC values were corrected with blanks and the typical uncertainties were 5 % for OC and 10 % for EC.

The second quarter of the filter was extracted in 15 mL of Milli-Q water (18 MΩ) with sonication for 30 min at temperature below 30 °C. The extracts were used for the determination of oxidative potential (Section 2.4) and of the water soluble organic and inorganic carbon (WSOC and WSIC). The latter using a Total Organic Carbon (TOC/TN) analyser (Shimadzu, model TOC-LCPH/CPN). The TOC protocol consisted in the injection of 50 μL of the solution into a combustion chamber to oxidize the total carbon (TC) into the sample that is detected as carbon dioxide by a non-dispersive infrared analyser (NDIR). A second aliquot of sample was injected after acidification and sparging steps, to produce a chemical conversion of inorganic carbon (carbonates and hydrogen carbonates, Inorganic Carbon, (IC) into carbon dioxide, which is directly revealed by NDIR. The organic portion is calculated as the difference of the two separate analysed parameters TC-IC. The final concentrations were blank corrected and the estimated typical uncertainty on WSOC was 10 %. WSIC ranged between 14 and 25 ng/m^3 (averages at the different typology of sites) in $PM_{2.5}$ and between 22 and 33 ng/m^3 in PM_{10}. The values were slightly lower than those (average of 68 ng/m^3 in $PM_{2.5}$) observed in the Brindisi industrial/harbour area (approximately 45 km NNW of Lecce) in Cesari et al. (2014). However, most of the values were under the limits of quantification so that this species was not furtherly investigated.

The third quarter of filter was extracted using 1.5 mL of Milli-Q water (18 MΩ) for two rounds (30 min each) in an ultrasonic bath. The extracts were used to determine the concentration of water soluble main ions by High-Performance Ion Chromatography (Dionex DX600 IC system – 125 μL injection loop). A Dionex IonPac AS23 analytical column (250 × 4 mm ID) was used, in isocratic mode with a Dionex IonPac AS23 guard column (50 × 4 mm ID), to separate the anions (NO_3^-, SO_4^{2-}, and $C_2O_4^{2-}$). The eluent used was 4.5 mM Na_2CO_3 and 1.1 mM $NaHCO_3$ with a flow rate of 1.0 mL/min. An analytical column (250 × 4 mm ID) made of Dionex IonPac CS12A was used to separate the cations (K^+, $NH4^+$, Ca^{2+}). Concentrations were calculated after blank subtraction. The typical uncertainties were between 5 % (K^+, Ca^{2+}, SO_4^{2-}, NO_3^-) and 10 % (NH_4^+ and $C_2O_4^{2-}$).

2.4. Determination of oxidative potential

The oxidative potential was determined using the DTT assay on extracts of the samples filtered using PTFE (0.45 μm pores) syringe filters to remove any suspended solids. The protocol used was adapted from that of Cho et al. (2005) and Chirizzi et al. (2017). Each filtered extract was incubated at 37 °C with Dhithiothreitol (DTT) (100 μM) in 0.1 M potassium phosphate buffer (PB) pH 7.4 and 5 mL of solution was used. An aliquot (0.5 mL) of the mixture was taken at specific times (in the range 0–45 min) adding 0.5 mL of 10 % trichloroacetic acid (TCA) to stop the reaction and 2 mL of 0.5 mM 5,5′-dithiobis(2-nitrobenzoic acid) (DTNB) in 0.4 M Tris-HCl (pH 8.9) containing 20 mM Ethylenediamine tetra-acetic acid (EDTA). The optical density absorption was measured using a UV–Vis spectrophotometer at 412 nm (UV–vis UV-1900i, Shimazdu Italia S.r.l., Milan). The rate of DTT consumption was determined from the measured optical density using the calibration of the spectrophotometer. Calibration was repeated for each series of 30 samples. In each series of 30 samples an analysis of at least three field was done. Final OP_V^{DTT} (in nmol/min m^3) was obtained after subtraction of blanks; the typical uncertainty, approximately 10 %, was determined by duplicating the determination of OP on a subset of samples (approximately one duplicate every ten analysis).

2.5. Statistical analysis and source apportionment approach

The seasonal and spatial variabilities of chemical compositions and source contributions were investigated for statistical significance by using the analysis of variance (ANOVA) test with a *p*-values threshold of 5 %. In this work when it is indicated a statistically significant difference or trends it means that it was obtained $p < 0.05$ while when it is indicated a negligible or limited variability it means that it is not statistically significant, i.e. $p > 0.05$.

The EPA PMF5 (Positive Matrix Factorization) receptor model, described in detail in Test S1 of supplementary material, was applied to identify the main natural and anthropogenic sources acting in the studied area, their chemical profiles and their contributions to the measured $PM_{2.5}$ and PM_{10} concentrations. PMF is one of the most used receptor model, in current research, to apportion the sources of particulate matter working with limited a priori information on sources (Belis et al., 2015; Barbaro et al., 2019; Hopke et al., 2020). PMF was run separately for $PM_{2.5}$ and PM_{10} with two datasets obtained pooling together samples collected at the different sites as done in other studies (Amato et al., 2016; Cesari et al., 2021). The input datasets were constructed including water soluble OC (WSOC) and water insoluble OC (WINSOC=OC-WSOC) instead of OC; in the same way, Ca was separated in water soluble (WSCa) and water insoluble (WINSCa) in order to try to better separate combustion and crustal sources. The strength of the input variables was classified using both, the Signal-to-Noise (S/N) criteria (Paatero and Hopke, 2003) and the percentage of data above the detection limits (Amato et al., 2016). The $PM_{2.5}$ (273 samples) and PM_{10} (98 samples) final input datasets included 24 chemical species with oxalate classified as bad (i.e. not used in PMF) and Cl classified as weak (i.e. uncertainties tripled in PMF run) for both size fractions.

Constraints were applied on the base solutions in order to improve the separation between some of the identified sources (Giannossa et al., 2022). The bootstrap methodology (Paatero et al., 2014) was applied to evaluate uncertainties in PMF results. The PMF was run considering $PM_{2.5}$ (or PM_{10}) as total variable. The best solutions in the base run identified seven factors/sources (sulphate, nitrate, marine, crustal, traffic, biomass burning, carbonates/construction) in both size fractions and the source industrial identified only in $PM_{2.5}$. Constrained runs were performed, for both size fractions, to improve the separation between some of the identified sources according to the experience of other studies in this area (Cesari et al., 2018; Giannossa et al., 2022) and based on maximise the load of specific tracers that mainly characterise the profiles according to the base run. The constraints used in PM_{10} were: pull up maximally K in biomass burning profile; Ti in crustal profile; and EC in traffic profile. The final dQ change, compared to the base run, was 2.8 %. The constraints used in $PM_{2.5}$ were: pull up maximally of K, WSOC, and Cl in biomass burning profile; of EC and WINSOC in traffic profile; pull down maximally of EC in crustal and sulphate profiles. The final dQ change, compared to the base run, was 7.2 %. These values of dQ are considered acceptable according to current scientific literature (Crova et al., 2024). The uncertainty was evaluated using the bootstrap of the constrained solutions calculated with 100 runs using random seed and $R = 0.6$ as threshold. Results showed no unmapped profiles for both size fractions. A good mapping of the solutions was obtained with some swaps for PM_{10} of sulphate with nitrate (7 %) and with marine (2 %). For $PM_{2.5}$, lower swaps were observed: 3 % between biomass burning and carbonates/construction; 2 % between traffic and sulphate; 2 % between traffic and crustal.

The evaluation of the contributions of the different sources to the OP_V^{DTT} was done with the methodology used in previous works (Liu et al., 2014; Cesari et al., 2019; Canha et al., 2024) based on the application of a multiple linear regression (MLR) analysis, assuming that the OP_V^{DTT} is linearly linked to the contribution of sources to mass concentrations, either $PM_{2.5}$ or PM_{10}. The equation used:

$$OP^{DTT}{}_V = M_{PM} \times \beta + \varepsilon \quad (1)$$

links the measured OP_V^{DTT} (dependent variable) expressed as a matrix (n × 1) in nmol/min·m^3 with M_{PM} that is a (n × p) matrix with the PM contributions (independent variables) attributed to each source by PMF5 in μg/m^3 and ε is the (n × 1) uncertainty matrix expressed in nmol/min·m^3. The symbol n represents the number of samples and the symbol p the number of sources. The estimator β is matrix (p × 1) that represents the slopes, expressed in nmol/min·μg. These slopes represent the intrinsic (i.e. mass normalsied) contributions of sources to the measured oxidative potential. MLR was applied using the XLSTAT tool setting the intercept equal to zero.

3. Results and discussion

3.1. Performance of the HSRS samplers during the campaign

The total number of expected samples during the campaign period was 387 and the final validated samples were 371 indicating an efficiency of 96 %. The number of samples loss for technical reasons (i.e. fault of solar panel, fault of the sampler and so on) were 14 corresponding to 3.5 % and 2 samples (0.5 %) were lost for incorrect handling. $PM_{2.5}$ and PM_{10} measured on monthly samples from HSRS samplers have been compared with the average values obtained from reference daily $PM_{2.5}$ and PM_{10} samples collected at the ECO observatory. The reference values were obtained with a SWAM dual channel (Fai instruments) low-volume (2.3 m^3/h) sampler detecting PM concentration through β-attenuation method and tested in a previous work (Conte et al., 2020). Results are reported in Fig. S1 showing the performance of HSRS sampler with good correlation with reference instrument, especially for $PM_{2.5}$. R^2 values were between 0.77 (PM_{10}) and 0.88 ($PM_{2.5}$). For both size fractions the slope was 0.95 and almost all measurements are within ± 10 % of the 1:1 line. The relative root mean squared error (RRMSE) was 11.6 % for PM_{10} and 8.6 % for $PM_{2.5}$. According to Li et al. (2013) the comparison with the reference instrument is excellent for $PM_{2.5}$ (i.e. RRMSE<10 %) and good for PM_{10} (i.e. 10 % < RRMSE<20 %).

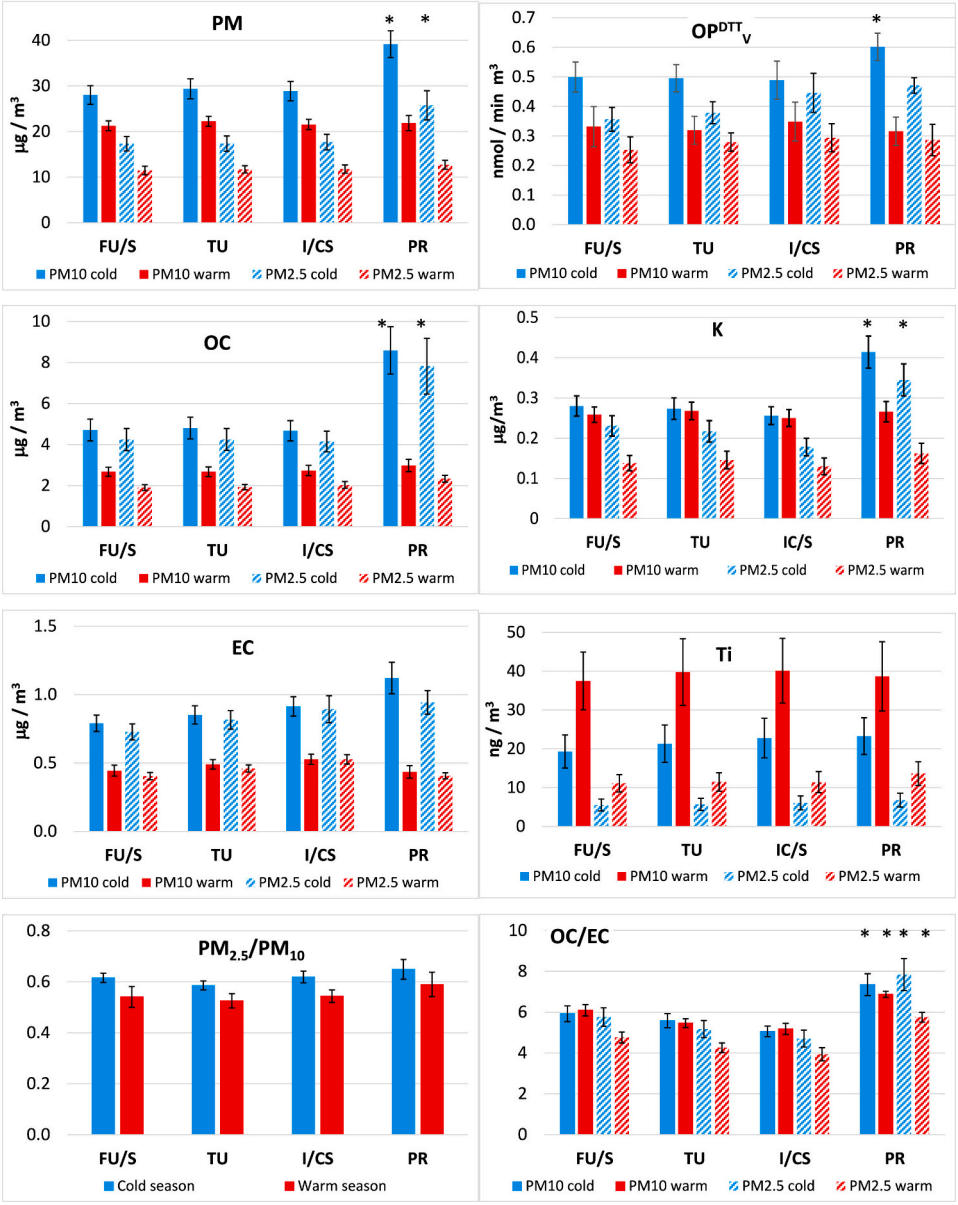

Fig. 2. Average values of PM, OC, EC, OP_V^{DTT}, K, Ti, $PM_{2.5}/PM_{10}$, and OC/EC in $PM_{2.5}$ and PM_{10} comparing the different typologies of sites and comparing cold and warm seasons. Error bars represent the standard errors. * Indicates a statistically significant spatial difference. Seasonal variabilities are statistically significant for PM, OC, EC, OP_V^{DTT}, Ti for both size fractions. K and OC/EC (limited to the $PM_{2.5}$ fraction), according to ANOVA test.

3.2. Variability of $PM_{2.5}$ and PM_{10} concentrations and chemical compositions

The average concentrations of the different chemical species (and min-max range) at the different typologies of sites are reported in Tables S2 (for $PM_{2.5}$) and S3 (for PM_{10}) showing not statistically significant difference among FU/S, TU, and IC/S sites in terms of yearly averages, according to the ANOVA test (Section 2.5); instead, concentrations at PR sites were larger, on average, compared to the other sites for both size fractions.

A deeper investigation of seasonal and spatial variability is reported in Figs. 2 and 3. Fig. 2 shows, for some selected species, the average concentrations at the different typologies of sites separated by cold (October–March) and warm seasons (April–September) for both $PM_{2.5}$ and PM_{10}. The PM concentrations showed a clear seasonal variability, statistically significant according to the ANOVA test, with larger values during the cold season compared to the warm season of approximately 38 % for PM_{10} and 54 % for $PM_{2.5}$ (averages of the area). During the cold season, the average values at PR sites are significantly larger than those at other typology of sites of approximately 28 % for PM_{10} and 32 % for $PM_{2.5}$. Instead, during the warm season, the spatial variability was not significant for both size fractions. Similar seasonal and spatial trends were also observed for OC (Fig. 2). Instead, EC had the same statistically significant seasonal variability discussed for OC with larger values during the cold period (of 89 % on average for PM_{10} and 85 % for $PM_{2.5}$) but the spatial variability was negligible, according to the ANOVA test. This trend suggests that, for all typologies of sites, there is a larger impact of combustion sources (i.e. road traffic and biomass burning) during the cold seasons for both size fractions. In addition, the ratio OC/EC (Fig. 2) is significantly larger (7.1 ± 0.5 for PM_{10} and 7.7 ± 0.4 for

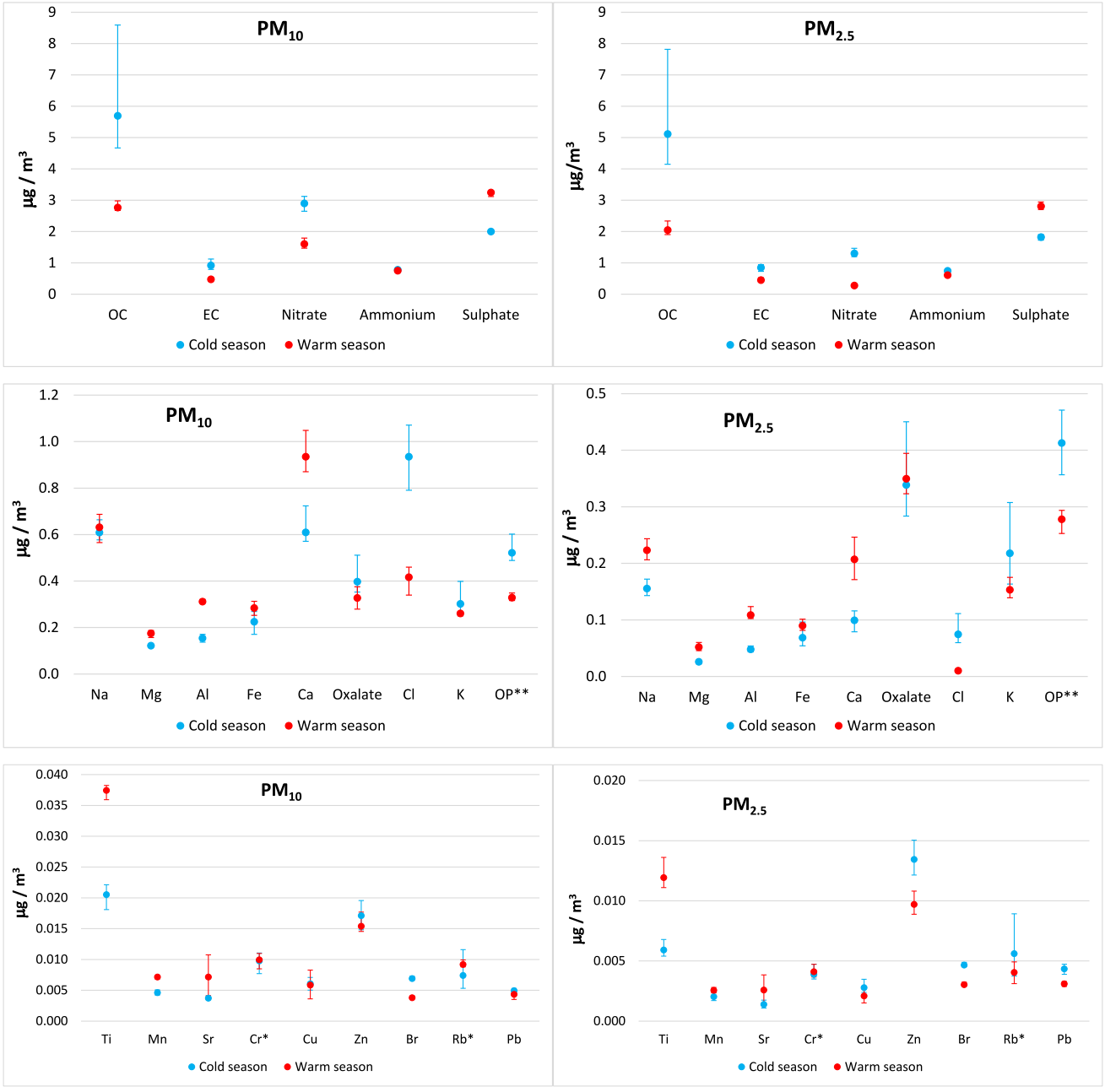

Fig. 3. Concentrations averaged over all the typology of sites separated for cold and warm seasons in $PM_{2.5}$ (right panels) and PM_{10} (left panels). The error bars represent the max-min values among the average of the different typology of sites. * concentration multiplied by 10. ** oxidative potential reported in nmol/min/m^3.

$PM_{2.5}$) at PR sites during cold seasons compared to the average of the other sites (5.9 ± 0.2 for PM_{10} and 4.5 ± 0.1 for $PM_{2.5}$). OC/EC is a useful diagnostic ratio furnishing information regarding the impact of combustion sources and the relative weight of biomass burning and road traffic (Sandrini et al., 2014. Escudero et al., 2015). The OC/EC ratio of road traffic emissions is typically between 0.3 and 5 with lower values for emissions of diesel vehicles and larger values for emissions of gasoline vehicles (Salameh et al., 2015; Amato et al., 2016). Values of OC/EC ranging between 5 and 12 were reported for biomass burning emissions (Szidat et al., 2006). The mentioned trends suggest that both road traffic and biomass burning sources affect all sites but in a different way, with a larger contribution of biomass burning at PR sites compared to the other typologies.

The spatial variability of K (Fig. 2) showed statistically significant (according to the ANOVA test) larger values (of about 48 % for PM_{10} and of 63 % for $PM_{2.5}$), during the cold season, at PR sites compared to the other typologies of sites. While negligible variability was observed during the warm period. This further corroborates the finding that PR sites are more impacted by biomass burning compared to the other sites considering that K, especially in the fine fraction, is an indicator of this source (Manousakas et al., 2022). Ti, instead has a limited spatial variability in both cold and warm seasons but a relevant seasonal variability with larger values during the warm (and dry season), thereby opposite to the seasonal trend of carbonaceous aerosol. This was likely due to large contributions of crustal resuspended dust during the warm seasons. Al and Ca had the same statistically significant seasonal trend (not shown), opposite to that of carbonaceous aerosol, with negligible spatial variability (on average).

The WSOC was very well correlated (Pearson coefficient 0.94) with OC for both size fractions (Fig. S2). The solubility of OC, calculated as the ratio WSOC/OC, was comparable in $PM_{2.5}$ and PM_{10}: average 68.1 % ± 0.9 % (standard error) in $PM_{2.5}$ and 67.1 % ± 1.3 % (standard error) in PM_{10}. In addition, the solubility did not show any statistically significant spatial variability while it was significantly larger (71.8 % ± 1.1 % in $PM_{2.5}$ and 72.7 % ± 1.4 % in PM_{10}) during the cold seasons compared to the average values (64.1 % ± 1.3 % in $PM_{2.5}$ and 60.9 ± 1.9 % in PM_{10}) observed during the warm seasons, according to the ANOVA test. High WSOC/OC ratios were observed during photochemical haze and in areas significantly affected by biomass burning (Decesari et al., 2006; Kumagai et al., 2009). The higher WSOC/OC ratio observed in winter compared to summer by Zhang et al. (2022) was interpreted as due to larger concentrations of soluble organic aerosol due to biomass burning. The trend observed here can therefore be due to larger concentrations of secondary organic aerosol observed in this area (Cesari et al., 2018) in this area and larger impact of biomass burning.

Fig. 3 compares the spatial variability (i.e. the min-max among the average values at the different typology of sites) with the seasonal variability separating cold and warm seasons for $PM_{2.5}$ and PM_{10}. It is observed that nitrate, EC, and Cl showed a seasonal variability with larger concentrations in the cold season and limited spatial variability, compared to the seasonal variability, in both size fractions. OC, K, Rb showed larger average values during the cold season and a spatial variability larger or comparable with the season one in both size fractions. Br, Pb showed again larger average values during the cold season with negligible spatial variability. Ammonium is fairly well distributed with negligible spatial and seasonal variability. Instead, sulphate has a seasonal variability with larger values during the warm season, opposite to nitrate and negligible spatial variability. This suggests that there is a decrease of ammonium nitrate in the fine fraction during the warm season (spring and summer) because of its thermal instability as observed in other studies (Querol et al., 2008; Pey et al., 2009). Ammonium sulphate (and bisulphate) dominates the secondary inorganic aerosol during the warm season in the fine fraction. Ti, Al, Fe, Mn, Ca, Sr, and Mg have larger average concentrations during the warm season and spatial variability is relevant only for Al, Ti, Ca, and Sr while Fe, Mn, and Mg have limited or negligible spatial variability on average. Na has larger concentrations during the warm season especially in the $PM_{2.5}$ fraction, instead in the PM_{10} fraction the spatial variability is larger than the seasonal one. Oxalate has larger spatial variability compared to the seasonal one in both size fractions.

3.3. Variability of oxidative potential

The OP_V^{DDT} and the corresponding values normalised by mass (OP_M^{DTT}) are reported (yearly averages) for the different typologies of sites and as average of all sites in Tables S2 ($PM_{2.5}$) and S3 (PM_{10}). Averages values, separated by cold and warm seasons, are shown in Fig. 2. A clear seasonal pattern was observed for both $PM_{2.5}$ and PM_{10} at all sites with larger values during the cold period compared to the warm one. The spatial variability was negligible during the warm period, instead, it was present during the cold period with larger values, on average, at the PR sites, according to the ANOVA test. This is analogue to the trend observed for OC and likely having the same drivers: larger contributions of combustion sources in the cold seasons and large contributions of biomass burning at the PR sites compared to the other sites.

The average values of PM, OP_V^{DDT}, and OP_M^{DDT} found for $PM_{2.5}$ and PM_{10} in this work are compared with the results of other studies in the same area, in Italy, and in Europe in Table 1. It must be said that a standard protocol for determining the oxidative potential with the DTT assay is not available and this leads to difficulties in comparing results obtained in different studies (Dominutti et al., 2025). However, Table 1 shows that the values reported here are in agreement with previous studies in the area done with different approaches and different time resolution. The OP_V^{DDT} are comparable with those observed in some of the other sites but lower than those observed in urban areas of north Italy and Europe. The variability shown in Table 1 suggests that OP^{DTT} is significantly depending on the details of the chemical composition rather than on the mass concentrations because areas with similar PM mass concentrations have significantly different OP values. This suggest that OP can be an indicator effectively complementary to the PM concentrations. The OP_V^{DDT} of $PM_{2.5}$ in this study represented, on average, 75.6 % of that of PM_{10} this is also in agreement with the results obtained in different sites. The OP_M^{DDT} is generally lower in PM_{10} compared to $PM_{2.5}$ suggesting that the oxidative potential of the coarse (i.e. $PM_{10-2.5}$) and of the fine ($PM_{2.5}$) fractions are influenced by different sources and processes leading to different intrinsic OP of the two size fractions (Giannossa et al., 2022; Grange et al., 2022).

3.4. Crustal enrichment factors

The crustal enrichment factors (EFs) give a useful information to identify the chemical species that have mainly a crustal origin (Zhang et al., 2008) helping in the interpretation of source apportionment based on receptor models because interpretation of source chemical profiles can benefit from knowledge if high-load species are of crustal, mixed, or anthropogenic origin (Ledoux et al., 2017; Tositti et al., 2014). The EF compares the concentration ratios of a specifical chemical species with a reference species in PM and in crustal material (Watson et al., 2002). The reference element chosen in this work is Al, but similar trends were observed also choosing Fe and this allows comparison with previous studies in this area (Contini et al., 2010; Cesari et al., 2012) and the composition of local resuspended soil was used as geological reference. Results are reported in Fig. 4, together with the relative abundances of the different chemical species in fine and coarse fraction, and they can be interpreted using the two-threshold method defined in Cesari et al. (2012) in which EF < 2 (threshold S_1) indicates a species with relevant crustal contribution; 2 < EF < 5 indicates a species with likely a mixed origin (i.e. limited enrichment with crustal material); EF > 5 (threshold S_2) indicates a species significantly enriched compared to local crustal dust. The average of the area is reported in Fig. 4 because there is not significant spatial variability in the interpretation of these results. The note nss- before the symbol of a chemical species indicates a value

Table 1
Comparison of average values of PM, OP_V^{DTT}, and OP_M^{DTT} found in this work with other studies in different sites in Italy and Europe dealing with simultaneous measurements of OP^{DDT} in $PM_{2.5}$ and PM_{10}.

$PM_{2.5}$ μg/m^3	OP_V^{DDT} nmol/min m^3	OP_M^{DTT} pmol/min μg	PM_{10} μg/m^3	OP_V^{DTT} nmol/min m^3	OP_M^{DTT} pmol/min μg	Notes	Reference
15.3	0.33	22.4	26.8	0.43	16.2	Yearly all sites, south Italy	This study
18.0	0.29	16.3	26.9	0.39	14.3	Yearly, Lecce IT (2016–2017)	Giannossa et al., 2022
21.8	0.21	11.0	30.8	0.23	8.0	39 daily samples, Lecce IT	Perrone et al., 2019
46.1	0.62	13.0	54.1	0.65	12.0	57 daily samples, Milan IT	Pietrogrande et al., 2022
–	0.33	28.0	–	0.43	–	(*) Yearly, Athens GR (2016–2017)	Paraskevopoulou et al., 2019
9.7	1.2	–	16.7	2.5	–	(**) Yearly, Barcelona ES (2018–2019)	in't Veld et al., 2023
5.7	0.4	–	7.9	0.5	–	(**) Yearly Montseny, ES rural site (2018–2019)	in't Veld et al., 2023
–	1.1	–	–	2.9	–	Bern CH	Weber et al., 2021
–	0.8	–	–	1.3	–	Zurich CH	Grange et al., 2022
–	0.7	–	–	1.0	–	Cadenazzo CH	Grange et al., 2022
–	0.6	–	–	0.8	–	Payerne CH	Grange et al., 2022
–	0.6	–	–	0.8	–	Basel CH	Grange et al., 2022
44.8	0.37	9.4	77.5	0.46	6.7	24 samples (3 h resolution) Belgrade, RS urban	Jovanovic et al., 2019

* Values for PM_{10} estimated as sum of coarse and fine fractions.
** Concentration in mass calculated from available tables in the paper.

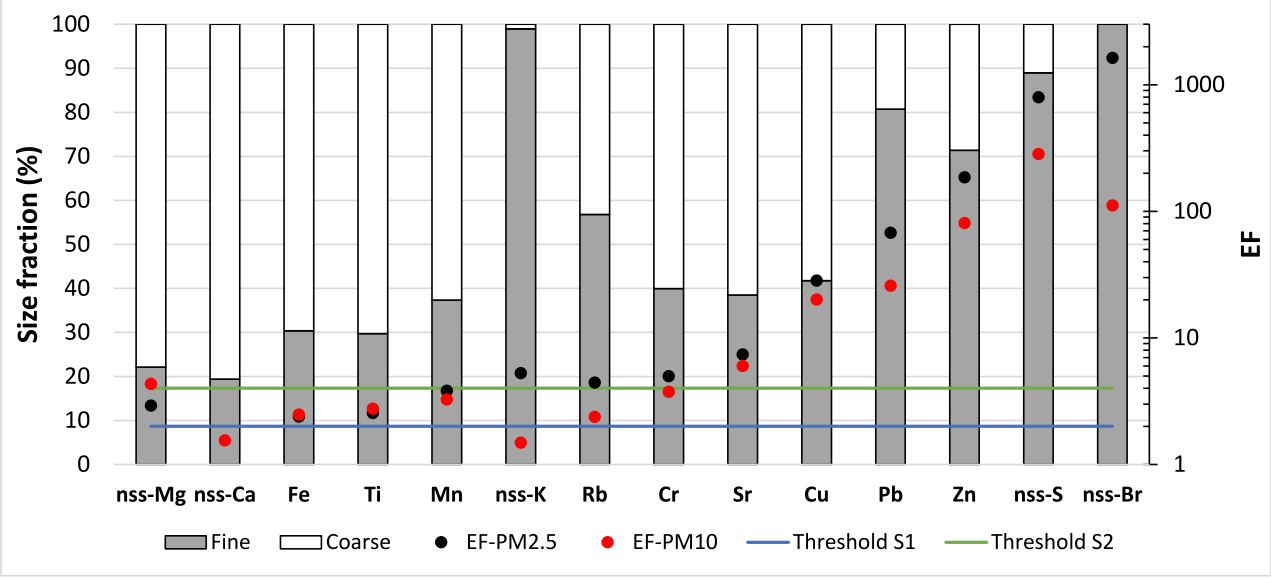

Fig. 4. Enrichment factors of $PM_{2.5}$ and PM_{10} (marks) and distribution of the different chemical species (bars) in fine ($PM_{2.5}$) and coarse ($PM_{2.5–10}$) fractions. The two horizontal lines are the threshold for identifying enriched (EFs > S_2), mixed (S_1 < EFs < S_2), and not enriched elements (EFs < S_1). The results are reported as average of all the typologies of sites.

referred to the non-sea-salt concentration of that species evaluated subtracting the expected values in sea salt calculated assuming that all Na was of marine origin. Cr, Sr, Cu, Pb, Zn, nss—S, nss-Br have a high enrichment suggesting a likely anthropogenic origin with enrichment generally larger in $PM_{2.5}$ compared to PM_{10}. Most of these species have a significance abundance (>50 %) in $PM_{2.5}$ suggesting anthropogenic sources significantly affecting fine particles. The species nss-K and Rb have a significant enrichment in $PM_{2.5}$ but are not enriched in PM_{10} and their abundance in $PM_{2.5}$ is larger than that in the coarse fraction. This suggests different origin of the two size fractions: mainly anthropogenic for the fine particles and essentially crustal for the coarse fraction. The species Mn, Ti, Fe, nss-Ca, and nss-Mg have mainly a crustal origin showing low or negligible enrichment comparable in $PM_{2.5}$ and PM_{10} and prevalent abundances (>50 %) in the coarse fraction.

3.5. *Source apportionment of $PM_{2.5}$ and PM_{10}*

The factors/sources chemical profiles, identified by the PMF5 for the two size fractions, are compared in Fig. 5. The profiles of $PM_{2.5}$ and PM_{10} are analogous, being characterised by similar target species, and allowed to individuate the same sources in the two size fractions with the exclusion of the industrial source that was identified only in $PM_{2.5}$.

The first factor, identified as traffic source, was characterised by EC, WINSOC and, to a lower extent, by Cr and Cu. The latter are two metals identified as significantly enriched. The second factor, identified as crustal source, was characterised by Al, Ti, WSCa, and, to a lower extent, by Mn, Fe that are all species with negligible or limited enrichment factors. This source was loaded with Rb in the PM_{10} profile but not in the $PM_{2.5}$ profile confirming possible multiple sources for this species as mention in Section 3.4. The third factor was identified with secondary nitrate; it is essentially a nitrate-rich source mainly characterised by NO_3^-. The fourth factor, identified as biomass burning source (BB), was

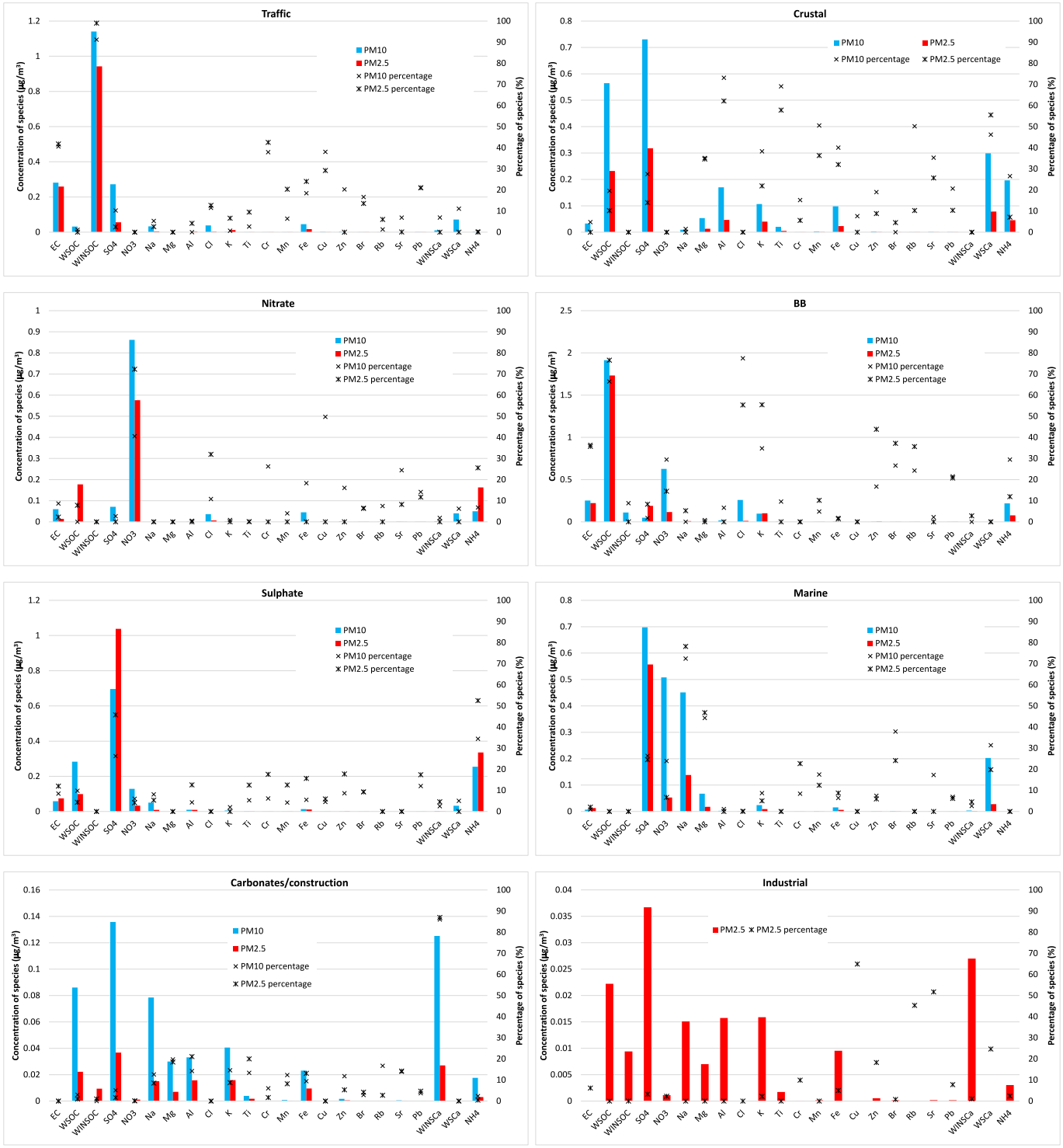

Fig. 5. Chemical profiles of the different factors/sources identified by the PMF5 for $PM_{2.5}$ and PM_{10}. Bars represent the concentrations of chemical species in each profile (left y-axis) and marks represent the percentage of each chemical species in the specific profile (right y-axis).

characterised by WSOC, Cl, K, and, to a lower extent, by EC, Zn, Br, and Rb (mainly for $PM_{2.5}$). The fifth factor was identified as sulphate-rich being characterised by SO_4^{2-} and NH_4^+. The ratios SO_4^{2-}/NH_4^+ in these profiles were 2.7 (PM_{10}) and 3.0 ($PM_{2.5}$) similar to the stoichiometric ratio (i.e. 2.66) of ammonium sulphate suggesting that secondary sulphate is an important component of this factor. The sixth factor was characterised by Na, Mg, and, to a lower extent by SO_4^{2-}, WSCa, NO_3^-, Br. The latter two species mainly for PM_{10}. This factor was identified as an aged marine contribution. This was expected in this area where strong chloride depletion of sea spray and formation of nitrate in the coarse fraction are typically observed especially during spring and summer period (Giannossa et al., 2022). The seventh factor was characterised by WINSCa and it was identified as a mixture of carbonates, also due to resuspended dust, and contributions from construction works. The eighth factor was identified only in $PM_{2.5}$ and it was a Cu-rich source loaded also of Rb and Sr. This was named industrial in this work even if its origin is not completely clear with the available dataset. The contribution of this source is very low, on average 1.3 % of $PM_{2.5}$.

It has to be observed that the use of WSOC and WINSOC allowed a better separation of the two combustion sources (i.e. traffic and biomass burning) because traffic seems to be associated mainly to the water insoluble fraction of OC, instead, biomass burning was associated to the water soluble fraction of OC. The ratio OC/EC in the traffic profile was 3.6 in $PM_{2.5}$ and 4.0 in PM_{10} in agreement with the typical values between 1.4 and 5 for gasoline catalyst vehicles and from 0.3 to 1 for diesel vehicles (Salameh et al., 2015; Amato et al., 2016). The OC/EC ratio in the biomass burning profile was larger compared to traffic profile and equal to 7.9 in $PM_{2.5}$ and 7.6 in PM_{10}. Again, results comparable to the values between 5 and 12 observed for biomass burning emissions (Szidat et al., 2006). The separation of the water insoluble and water soluble fractions of Ca allowed a better separation between crustal source, mainly characterised by soluble Ca, and carbonates/construction source that seems to be characterised mainly by insoluble Ca.

Results are reported in Fig. 6 in terms of absolute contributions to $PM_{2.5}$ and PM_{10} separately for the different typologies of sites. Fig. S5 shows the same analysis in terms of relative contributions and Fig. S6 compares the absolute contributions to $PM_{2.5}$ and PM_{10}, averaged over all sites, showing the influence of the different sources to the fine and coarse particles. The most contributing sources are traffic and biomass burning that appears comparable in several sites. These two combustion-related sources explain between 45 % and 50 % of $PM_{2.5}$ and between 45 % and 60 % of PM_{10}. Sulphate and nitrate are the successive relevant sources, with sulphate significantly larger than nitrate in $PM_{2.5}$ but comparable in PM_{10}. These two sources, that better represent secondary inorganic aerosol, represent between 35 % and 42 % of $PM_{2.5}$ at the different typologies of sites and between 32 % and 41 % of PM_{10}.

The most evident spatial variability is represented by the largest contributions of biomass burning at PR sites for both $PM_{2.5}$ and PM_{10}.

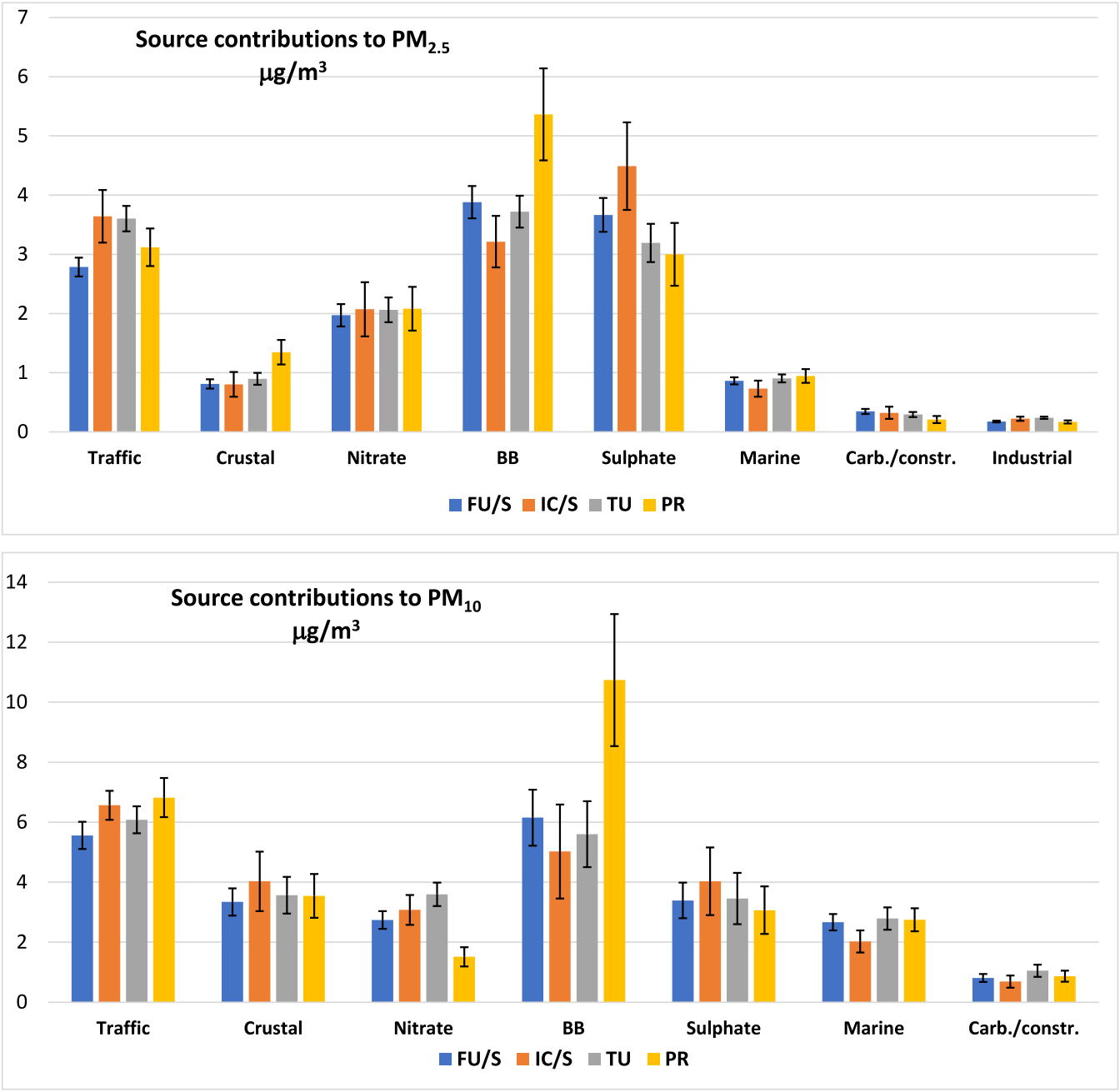

Fig. 6. Absolute average contributions (and standard errors) of the different factors/sources identified by the PMF5 to $PM_{2.5}$ and PM_{10} at the different typology of sites.

Traffic contribution is slightly lower at FU/S sites in both size fractions. Crustal and marine contributions have limited spatial variability in the size fraction in which they are more abundant (i.e. PM_{10}). Nitrate shows a uniform spatial distribution, on average, in $PM_{2.5}$, however, in PM_{10} the PR sites show lower contributions compared to the other typologies of sites. Carbonates/construction source is quite uniform in both size fractions, however, in PM_{10} it is possible to observe slightly larger values at TU sites. A deeper investigation of this source showed local contributions at a specific site (i.e. the traffic site S9) as shown in Fig. S7. The figure shows the contribution of carbonates/construction source at site S9 and the average of the area surrounding this site. In PM_{10} it is observed a significantly larger contribution at site S9 in the period February–August 2022 that is approximately the period in which there have been large renovation work of the exterior of a public building very near the sampling location. This is the reason why this source has been labelled carbonates/construction. Fig. S7 also shows that WINSCa has the same trend as the source identified by PMF5 and that this trend is not visible on $PM_{2.5}$ confirming that is a contribution to coarse particles.

The spatial variability (i.e. the min-max among the average at the different typology of sites) of the contributions of the different sources to $PM_{2.5}$ and PM_{10} is compared with the seasonal variability, dividing cold and warm seasons in Fig. S8. Traffic, biomass burning and nitrate shows a seasonal variability with larger values during winter for both size fractions. The spatial variability is relevant for traffic and biomass burning, instead, nitrate shows a non-negligible spatial variability only for PM_{10}. This corroborates the finding, discussed previously, that nitrate in fine and coarse fraction originate from different sources/process. This result agrees with the results of a previous study at the site S1 (Cesari et al., 2021). Crustal has a seasonal variability more important than the spatial one with larger values observed during the warm season. This is likely due to the dryness of soil during the warm season that favours resuspension of dust. Marine and industrial (only $PM_{2.5}$) do not show significant seasonal or spatial variabilities on average terms. Carbonates/construction in PM_{10} are larger during the warm season and present a slight spatial variability, likely related to the local construction sources previously mentioned. Sulphate source shows larger contributions during warm season in $PM_{2.5}$ with significant spatial variability. Instead, in PM_{10}, the seasonal variability is lower even if there is a non-negligible spatial variability. This behaviour is different from that discussed for the chemical species ammonium and sulphate (Section 3.2) and suggest that the sulphate-rich source found by PMF5 is not completely comparable to secondary ammonium sulphate and it is possible to have contributions from anthropogenic sources because the profiles include loads of some metals and also of secondary organics confirmed by the presence of WSOC in the profiles (Fig. 5).

3.6. Comparison of PMF5 apportionment with mass closure

Some of the sources found by the application of PMF5 receptor model can be compared to results obtainable by the analysis of measured concentrations (that we indicate here as mass closure) based on a few specific assumptions on the origin of chemical species considered tracers/indicator of natural and anthropogenic sources (Giannossa et al., 2022).

Marine contribution can be evaluated considering all Na coming from sea salt and the typical ratio Cl/Na = 1.81 of sea water (Marenco et al., 2006) so that the contribution of this source can be evaluated as 2.81Na. This formula, based only on Na, limit the problem due to chloride depletion that is relevant in the summer in this area (Cesari et al., 2018). The non-sea-salt sulphate was evaluated as nss-SO_4^{2-} = SO_4^{2-}- 0.25Na. The secondary sulphate was evaluated as the sum of nss-SO_4^{2-} and NH_4^+. The crustal contribution was calculated as 1.15 (1.89Al + 2.14Si + 1.67Ti + 1.4WINSCa + 1.2WINSK + 1.36 Fe) that consider metal oxides of Al, Si and Fe, plus the insoluble fraction (WINS) of K and Ca (Giannossa et al., 2022). Si was not directly measured but evaluated as Si = 2.65 Al. Carbonates were calculated from non-sea-salt calcium and magnesium as 1.5 nss-Ca + 2.5 nss-Mg (Perrino et al., 2014).

The comparison of results of these calculations with the contributions evaluated using PMF5 are reported in Fig. S3. There is a reasonable agreement for marine contribution in both size fractions even if slightly larger values are obtained by PMF5 (an average difference over all sites of 0.5 μg/m^3 in PM_{10} and 0.3 μg/m^3 in $PM_{2.5}$), likely because the profile of the receptor model includes also a part due to aged marine aerosol represented by the presence of nitrate, i.e. formation of sodium nitrate. This is mainly evident in the PM_{10} profile and it was observed also in other studies in this area (Giannossa et al., 2022). The agreement for sulphate is good (i.e. differences within the error bars) for PM_{10} while a slight overestimation of PMF5 in $PM_{2.5}$ (on average of 0.6 μg/m^3) was visible for $PM_{2.5}$ mainly at IC/S and FU/S sites. This could be due to the presence of WSOC and some metals in the sulphate profile confirming the possible mixing of this source with anthropogenic and/or secondary organics sources as mentioned in Section 3.5. Regarding crustal and carbonates/construction sources, the agreement is good for $PM_{2.5}$ (i.e. differences within the error bars). However, for the PM_{10} where these sources are more relevant in both absolute and relative terms, it was observed a certain overestimation of carbonates/contractions (on average of 0.4 μg/m^3) of PMF5 and a slight underestimation of crustal (approximately 0.5 μg/m^3 on average). It is interesting to observe that the agreement was better (i.e. differences within the errors bars) for the sum of these two sources. This suggests that it could be present a certain level of mixing in the profiles of these sources, not surprising considering the potential collinearity in the source profiles due to the similarity and correlations of the chemical tracers/indicators of these sources.

3.7. Source apportionment of OP_V^{DTT}

The contributions of the sources identified by the PMF5 to OP_V^{DTT} in the two size fractions was obtained by MLR analysis (Section 2.5). Only four sources, i.e. traffic, biomass burning, sulphate, and crustal were giving contributions statistically significant ($p < 0.05$ in the MLR). The fitting coefficients for these sources are reported in Table S4 for both size fractions. The comparison between OP_V^{DTT} measured and reconstructed by PMF5-MLR is reported in Fig. S3. The absolute average contribution to OP_V^{DTT} in the two size fractions of the different typology of sites are reported in Fig. 7. Fig. S9 shows the same analysis in terms of relative contributions and Fig. S10 compares the absolute contributions to OP_V^{DTT}, averaged over all sites, showing the influence of the different sources to the oxidative potential of $PM_{2.5}$ and PM_{10}.

Contributions of all sources but crustal one gave larger contributions to OP_V^{DTT} to $PM_{2.5}$ compared to that to the coarse fraction (i.e. $PM_{10-2.5}$). The relative contribution of sulphate-rich source to OP_V^{DTT} is, on average, the same to $PM_{2.5}$ and PM_{10} suggesting that coarse sulphate is not redox active. This is a results comparable at the different sites and is it coherent with the findings of a previous study at site S1 (Giannossa et al., 2022). The most contributing source is traffic followed by biomass burning. At PR sites the absolute contributions of these two sources are comparable in both size fractions. The total contribution of these two sources ranges from 56.6 % (IC/S sites) to 68.7 % (TU sites) in $PM_{2.5}$ and from 61.8 % (FU/S) to 75.3 % (PR sites) in PM_{10}. Contribution of crustal source is low in $PM_{2.5}$ (on average 4 %) but non negligible in PM_{10} (on average 10.8 %). Nitrate does not have a statistically significant contribution to OP_V^{DTT} in this dataset and the contributions of sulphate-rich source ranged between 22 % (at PR sites) to 33 % (FU/S and IC/S sites) in $PM_{2.5}$ and between 17.9 % (PR sites) to 26.5 % (IC/S). This suggests that contributions to OP_V^{DTT} of secondary inorganic aerosol may be partially due to the mixing of chemical profiles in PMF5 (not characterised only by nitrate, sulphate, and ammonium) but that are anyway significantly lower than the contributions of these sources to mass concentrations.

The spatial variability (i.e. the min-max among the average at the different typology of sites) of the contributions of the different sources to OP_V^{DTT} is compared with the seasonal variability for the two size fractions, separating cold and warm seasons, in Fig. S11. Traffic and biomass

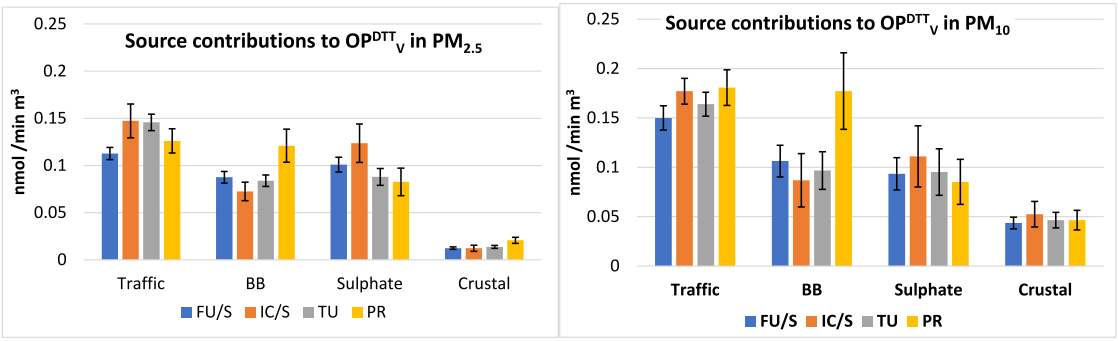

Fig. 7. Absolute average contributions (and standard errors) of the different factors/sources identified by the PMF5 to OP_V^{DTT} of $PM_{2.5}$ and PM_{10} at the different typology of sites. Error bars represent the standard errors.

burning have larger contributions during the cold season with significant spatial variability, especially during the cold season for biomass burning. Crustal contributions to OP_V^{DTT} are larger during the warm seasons, as it was observed for mass contributions, but showed negligible spatial variability. Sulphate-rich source contributions have a seasonal variability with larger values during the warm season and present spatial variability in $PM_{2.5}$, however, in PM_{10} the contributions to OP_V^{DTT} are rather uniform during the season and for the different typology of sites. This is comparable to what has been observed for contributions to mass concentrations (Section 3.6).

4. Conclusions

An analysis of spatial and seasonal variabilities of concentration, chemical composition, and oxidative potential of $PM_{2.5}$ and PM_{10} has been performed simultaneously at 22 sites, of different typology, in the central Mediterranean area of Lecce located in south Italy. Source apportionment with the PMF5 receptor model coupled with MLR analysis was used to investigate the role of the main natural and anthropogenic sources to PM concentration and to its oxidative potential.

Results show that the HSRS smart samplers used, even if operated at low temporal resolution, were suitable to reach the objectives of the study. The source apportionment highlighted the contributions of eight sources: traffic, biomass burning, sulphate-rich, nitrate, crustal, marine, carbonates/construction, and industrial. The latter only in $PM_{2.5}$ representing approximately 1.3 % of $PM_{2.5}$. The use of water soluble and insoluble fractions of OC in the input of receptor model allowed a better separation of the two combustion-related sources (i.e. traffic and biomass burning) because WINSOC was mainly associated to traffic while WSOC was associated to biomass burning. These two sources represented 45 %–50 % of $PM_{2.5}$, on average, at the different typologies of sites and 45 %–60 % of PM_{10}. Both sources have a seasonal variability with larger values in the cold season and present a relevant spatial variability with low traffic contribution at FU/S sites, compared to the other typologies of sites, and larger contributions of biomass burning at PR sites.

The use of water soluble and insoluble fractions of Ca in the PMF5 input allowed to identify and separate carbonates/construction source (mainly characterised by WINSCa) from crustal source (mainly characterised by WSCa).

Nitrate and sulphate-rich sources are those better representing secondary inorganic aerosol and they represent 35 %–42 % of $PM_{2.5}$ and 32–41 % of PM_{10}. Nitrate and sulphate-rich have opposite seasonal trends. Nitrate was larger during cold seasons with negligible spatial variability and sulphate was larger during warm season with a non-negligible spatial variability. Results found showed that the sulphate-rich sources found by PMF5 was not completely comparable to secondary ammonium sulphate and it included some contributions from anthropogenic sources having a profile loaded with metals and with WSOC. In general, chemical compositions and source contributions showed a seasonal variability larger than the spatial variability with the exclusions of traffic and biomass burning.

OP_V^{DTT} showed negligible spatial variability during the warm period but significant variability during the cold season due to the contributions of biomass burning. OP_V^{DTT} was, on average, larger during the cold seasons in both size fractions. The OP_V^{DTT} in $PM_{2.5}$ represented between 73 % (FU/S sites) and 90 % (IC/S sites) of the average values in PM_{10}.

The sources that gave contributions statistically significant to OP_V^{DTT} were (in descendent order for contributions) traffic, biomass burning, sulphate-rich, and crustal for both size fractions. The most contributing source was traffic followed by biomass burning with the exception of PR sites where the contributions of these two sources were comparable in both size fractions. The total contribution of these two sources ranged from 56.6 % (IC/S sites) to 68.7 % (TU sites) in $PM_{2.5}$ and from 61.8 % (FU/S) to 75.3 % (PR sites) in PM_{10}. Contribution of crustal source was low in $PM_{2.5}$ (on average 4 %) but non negligible in PM_{10} (on average 10.8 %) with higher contributions during the warm season compared to the cold season. The contributions of sulphate-rich source ranged between 22 % (at PR sites) to 33 % (FU/S and IC/S sites) in $PM_{2.5}$ and between 17.9 % (PR sites) to 26.5 % (IC/S) with higher contributions during cold season compared to warm season. The contributions to OP_V^{DTT} of secondary inorganic aerosol may be partially due to the mixing of chemical profiles in PMF5, however, these are significantly lower than the contributions to mass concentrations.

CRediT authorship contribution statement

Serena Potì: Writing – review & editing, Formal analysis, Data curation, Conceptualization. **Eva Merico:** Writing – review & editing, Investigation, Formal analysis, Data curation. **Marianna Conte:** Writing – review & editing, Conceptualization. **Florin Unga:** Writing – review & editing, Data curation. **Daniela Cesari:** Writing – review & editing, Formal analysis, Data curation. **Adelaide Dinoi:** Writing – review & editing, Data curation. **Anna Rita De Bartolomeo:** Formal analysis, Data curation. **Antonio Pennetta:** Writing – review & editing, Formal analysis, Data curation. **Ermelinda Bloise:** Writing – review & editing, Formal analysis, Data curation. **Giuseppe Deluca:** Formal analysis, Data curation. **Roberto Ferrera:** Investigation, Data curation. **Enrico Bompadre:** Investigation, Data curation. **Maria Rachele Guascito:** Writing – review & editing, Formal analysis, Data curation, Conceptualization. **Daniele Contini:** Writing – original draft, Funding acquisition, Conceptualization.

Declaration of competing interest

The authors declare that they have no known competing financial interests or personal relationships that could have appeared to influence the work reported in this paper.

Acknowledgements

This research was supported by the project IR0000032 – ITINERIS, Italian Integrated Environmental Research Infrastructures System (D.D. n. 130/2022 - CUP B53C22002150006) Funded by EU - Next Generation EU; PNRR - Mission 4 “Education and Research” - Component 2: “From research to business” - Investment 3.1: “Fund for the realisation of an integrated system of research and innovation infrastructures”. Authors wish to thank Dr. A. Carlino (University of Salento) for his help in performing the chemical analysis. Authors wish to acknowledge the support for hosting the instruments and providing electrical power of: S. Francioso e G. Corsini (Provincia di Lecce); G. Molendini and D. Pareo (Municipality of Lecce); F. Papadia (Municipality of Aradeo); L. Giotta (University of Salento); Soprintendenza archeologia belle arti e paesaggio per le province di Brindisi e Lecce; secondary high school “A. Galateo”; scientific high school “C. De Giorgi”; scientific high school “G. Banzi Bazoli”; technical and professional institute “A. De Pace”; Technical Institute “G. Deledda”; Technical Institute “Presta Columella”; V. Morelli (Armafer s.r.l.); A. Giannone (Klepierre – Commercial Center Cavallino); A. Epifani (Enel Italia S.p.A.); S. Fonte (Autosat S.p.A.); M.G. Manco and A. Russo.

Appendix A. Supplementary data

Supplementary data to this article can be found online at https://doi.org/10.1016/j.scitotenv.2025.179283.

Data availability

Data will be made available on request.

References

Amato, F., Alastuey, A., Karanasiou, A., Lucarelli, F., Nava, S., Calzolai, G., Severi, M., Becagli, S., Vorne, L.G., Colombi, C., Amato, F., Alastuey, A., Karanasiou, A., Lucarelli, F., Nava, S., Calzolai, G., Severi, M., Becagli, S., Vorne, L.G., Colombi, C., Alves, C., Custodio, D., Nunes, T., Cerqueira, M., Pio, C., Eleftheriadis, K., Diapouli, E., Reche, C., Minguillon, M.C., Manousakas, M.I., Maggos, T., Vratolis, S., Harrison, R.M., Querol, X., 2016. AIRUSE-LIFEC: a harmonized PM speciation and source apportionment in five southern European cities. Atmos. Chem. Phys. 16, 3289–3309.

Barbaro, E., Feltracco, M., Cesari, D., Padoan, S., Zangrando, R., Contini, D., Barbante, C., Gambaro, A., 2019. Characterization of the water soluble fraction in ultrafine, fine, and coarse atmospheric aerosol. Sci. Total Environ. 658, 1423–1439.

Basagaña, X., Jacquemin, B., Karanasiou, A., Ostro, B., Querol, X., Agis, D., et al., 2015. Short-term effects of particulate matter constituents on daily hospitalizations and mortality in five South-European cities: results from the MED-PARTICLES project (on behalf of the MED-PARTICLES Study group). Environ. Int. 75, 151–158.

Bates, J.T., Fang, T., Verma, V., Zeng, L., Weber, R.J., Tolbert, P.E., Russell, A.G., 2019. Review of acellular assays of ambient particulate matter oxidative potential: methods and relationships with composition, sources, and health effects. Environ. Sci. Technol. 53 (8), 4003–4019.

Belis, C.A., Karagulian, F., Amato, F., Almeida, M., Artaxo, P., Beddows, D.C.S., Bernardoni, V., Bove, M.C., Carbone, S., Cesari, D., Contini, D., Cuccia, E., Diapouli, E., Eleftheriadis, K., Favez, O., El Haddad, I., Harrison, R.M., Hellebust, S., Hovorka, J., Jang, E., Jorquera, H., Kammermeier, T., Karl, M., Lucarelli, F., Mooibroek, D., Nava, S., Nøjgaard, J.K., Paatero, P., Pandolfi, M., Perrone, M.G., Petit, J.E., Pietrodangelo, A., Pokornà, P., Prati, P., Prevot, A.S.H., Quass, U., Querol, X., Saraga, D., Sciare, J., Sfetsos, A., Valli, G., Vecchi, R., Vestenius, M., Yubero, E., Hopke, P.K., 2015. A new methodology to assess the performance and uncertainty of source apportionment models II: the results of two European intercomparison exercises. Atmos. Environ. 123 (Part A), 240–250.

Canha, N., Gonçalves, S., Sousa, D., Gamelas, C., Mendez, S., Cabo Verde, S., Almeida, S. M., De Bartolomeo, A.R., Guascito, M.R., Merico, E., Contini, D., 2024. Pollution sources affecting the oxidative potential of fine aerosols in a Portuguese urban-industrial area-an exploratory study. Air Qual. Atmos. Hlth 17 (9), 2005–2015.

Cavalli, F., Viana, M., Yttri, K.E., Genberg, J., Putaud, J.P., 2010. Toward a standardised thermal-optical protocol for measuring atmospheric organic and elemental carbon: the EUSAAR protocol. Atmos. Meas. Tech. 3, 79–89.

Cesari, D., Contini, D., Genga, A., Siciliano, M., Elefante, C., Baglivi, F., Daniele, L., 2012. Analysis of raw soils and their re-suspended PM10 fractions: characterisation of source profiles and enrichment factors. Appl. Geochem. 27, 1238–1246.

Cesari, D., Genga, A., Ielpo, P., Siciliano, M., Mascolo, G., Grasso, F.M., Contini, D., 2014. Source apportionment of PM2. 5 in the harbour–industrial area of Brindisi (Italy): identification and estimation of the contribution of in-port ship emissions. Sci. Total Environ. 497, 392–400.

Cesari, D., Merico, E., Dinoi, A., Marinoni, A., Bonasoni, P., Contini, D., 2018. Seasonal variability of carbonaceous aerosols in an urban background area in southern Italy. Atmos. Res. 97-108, 0169–8095.

Cesari, D., Merico, E., Grasso, F.M., Decesari, S., Belosi, F., Manarini, F., De Nuntiis, P., Rinaldi, M., Volpi, F., Gambaro, A., Morabito, E., Contini, D., 2019. Source apportionment of PM2.5 and of its oxidative potential in an industrial suburban site in South Italy. Atmosphere 10 (12), 758.

Cesari, D., Merico, E., Grasso, F.M., Dinoi, A., Conte, M., Genga, A., Siciliano, M., Petralia, E., Stracquadanio, M., Contini, D., 2021. Analysis of the contribution to PM10 concentrations of the largest coal-fired power plant of Italy in four different sites. Atmos. Pollut. Res. 12 (8), 101135.

Chirizzi, D., Cesari, D., Guascito, M.R., Dinoi, A., Giotta, L., Donateo, A., et al., 2017. Influence of Saharan dust outbreaks and carbon content on oxidative potential of water-soluble fractions of PM2.5 and PM10. Atmos. Environ. 163, 1–8.

Cho, A.K., Sioutas, C., Miguel, A.H., Kumagai, Y., Schmitz, D.A., Singh, M., et al., 2005. Redox activity of airborne particulate matter at different sites in the Los Angeles Basin. Environ. Res. 99, 40–47.

Conte, M., Contini, D., 2019. Size-resolved particle emission factors of vehicular traffic derived from urban eddy covariance measurements. Environ. Pollut. 251, 830–838.

Conte, M., Merico, E., Cesari, D., Dinoi, A., Grasso, F.M., Donateo, A., Guascito, M.R., Contini, D., 2020. Long-term characterisation of African dust advection in south-eastern Italy: influence on fine and coarse particle concentrations, size distributions, and carbon content. Atmos. Res. 233, 104690.

Contini, D., Genga, A., Cesari, D., Siciliano, M., Donateo, A., Bove, M.C., Guascito, M.R., 2010. Characterisation and source apportionment of PM10 in an urban background site in Lecce. Atmos. Res. 95 (1), 40–54.

Crova, F., Bernardoni, V., Cadeo, L., Canepari, S., Hopke, P.K., Massimi, L., Perrino, C., Valli, G., Vecchi, R., 2024. Multi-time and multi-size resolution receptor modeling to exploit jointly atmospheric aerosol data measured at different time resolutions and in multiple size classes. Atmos. Environ. 333, 120672.

Daellenbach, K.R., Uzu, G., Jiang, J., Cassagnes, L.-E., Leni, Z., Vlachou, A., et al., 2020. Sources of particulate-matter air pollution and its oxidative potential in Europe. Nature 2020 (587), 414–419.

Decesari, S., Fuzzi, S., Facchini, M.C., Mircea, M., Emblico, L., Cavalli, F., Maenhaut, W., Chi, X., Schkolnik, G., Falkovich, A., Rudich, Y., Claeys, M., Pashynska, V., Vas, G., Kourtchev, I., Vermeylen, R., Hoffer, A., Andreae, M.O., Tagliavini, E., Moretti, F., Artaxo, P., 2006. Characterization of the organic composition of aerosols from, Rondonia, Brazil, during the LBA–SMOCC 2002 experiment and its representation through model compounds. Atmos. Chem. Phys. 6, 375–402.

Dinoi, A., Gulli, D., Weinhold, K., Ammoscato, I., Calidonna, C.R., Wiedensohler, A., Contini, D., 2023. Characterization of ultrafine particles and the occurrence of new particle formation events in an urban and coastal site of the Mediterranean area. Atmos. Chem. Phys. 23, 2167–2181.

Dinoi, A., Pavese, G., Calvello, M., Chirizzi, D., Pennetta, A., De Benedetto, G.E., Esposito, F., Mapelli, C., Contini, D., 2024. Characterization of aerosol and its oxidative potential in a coastal semi-rural site of southern Italy. Atmos. Res. 333, 120656.

Dominutti, P.A., Borlaza, L.J.S., Sauvain, J.J., Thuy, V.D.N., Houdier, S., Suarez, G., Jaffrezo, J.L., Tobin, S., Trébuchon, C., Socquet, S., Moussu, E., Mary, G., Uzu, G., 2023. Source apportionment of oxidative potential depends on the choice of the assay: insights into 5 protocols comparison and implications for mitigation measures. Environ. Sci.: Atmos. 3, 1497.

Dominutti, P.A., Jaffrezo, J.-L., Marsal, A., Mhadhbi, T., Elazzouzi, R., Rak, C., Cavalli, F., Putaud, J.-P., Bougiatioti, A., Mihalopoulos, N., Paraskevopoulou, D., Mudway, I.S., Nenes, A., Daellenbach, K.R., Banach, C., Campbell, S.J., Cigánková, H., Contini, D., Evans, G., Georgopoulou, M., Ghanem, M., Glencross, D. A., Guascito, M.R., Herrmann, H., Iram, S., Jovanović, M., Jovašević-Stojanović, M., Kalberer, M., Kooter, I.M., Paulson, S.E., Patel, A., Perdrix, E., Pietrogrande, M.C., Mikuška, P., Sauvain, J.-J., Seitanidi, A., Shahpoury, P., Souza, E.J.S., Steimer, S., Stevanovic, S., Suarez, G., Subramanian, P.S.G., Utinger, B., van Os, M.F., Verma, V., Wang, X., Weber, R.J., Yang, Y., Querol, X., Hoek, G., Harrison, R.M., Uzu, G., 2025. An interlaboratory comparison to quantify oxidative potential measurement in aerosol particles: challenges and recommendations for harmonisation. Atmos. Meas. Tech. 18, 177–195.

Escudero, M., Viana, M., Querol, X., Alastuey, A., Díez, Hernández P., García Dos Santos, S., Anzano, J., 2015. Industrial sources of primary and secondary organic aerosols in two urban environments in Spain. Environ. Sci. Pollut. Res. 22, 10413–10424.

Giannossa, L.C., Cesari, D., Merico, E., Dinoi, A., Mangone, A., Guascito, M.R., Contini, D., 2022. Inter-annual variability of source contributions to PM10, PM2.5, and oxidative potential in an urban background site in the Central Mediterranean. J. Environ. Manage. 319, 115752.

Grange, S.K., Uzu, G., Weber, S., Jaffrezo, J.-L., Hueglin, C., 2022. Linking Switzerland’s PM_{10} and $PM_{2.5}$ oxidative potential (OP) with emission sources. Atmos. Chem. Phys. 22, 7029–7050.

Guascito, M.R., Lionetto, M.G., Mazzotta, F., Conte, M., Giordano, M.E., Caricato, R., De Bartolomeo, A.R., Dinoi, A., Cesari, D., Merico, E., Mazzotta, L., Contini, D., 2023. Characterisation of the correlations between oxidative potential and in vitro biological effects of PM10 at three sites in the Central Mediterranean. J. Hazard. Mater. 448, 130872.

Hopke, P.K., Dai, Q., Li, L., Feng, Y., 2020. Global review of recent source apportionments for airborne particulate matter. Sci. Total Environ. 740, 140091.

Jiang, H., Ahmed, C.M.S., Canchola, A., Chen, Y.J., Lin, Y.H., 2019. Use of dithiothreitol assay to evaluate the oxidative potential of atmospheric aerosols. Atmosphere 10, 571.

Jovanovic, M.V., Savic, J.Z., Salimi, F., Stevanovic, S., Brown, R.A., Jovasevic-Stojanovic, M., Manojlovic, D., Bartonova, A., Bottle, S., Ristovski, Z.D., 2019. Measurements of oxidative potential of particulate matter at belgrade tunnel; Comparison of BPEAnit, DTT and DCFH Assays. Int. J. Environ. Res. Public Health 16 (24), 4906.

Kelly, F.J., Fuller, G.W., Walton, H.A., Fussell, J.C., 2012. Monitoring air pollution: use of early warning systems for public health. Respirology 17 (1), 7–19.

Kumagai, K., Iijima, A., Tago, H., Tomioka, A., Kozawa, K., Sakamoto, K., 2009. Seasonal characteristics of water–soluble organic carbon in atmospheric particles in the inland Kanto plain, Japan. Atmos. Environ. 43, 3345–3351.

Ledoux, F., Kfoury, A., Delmaire, G., Roussel, G., El Zein, A., Courcot, D., 2017. Contributions of local and regional anthropogenic sources of metals in PM2.5 at an urban site in northern France. Chemosphere 181, 713–724.

Li, M.F., Tang, X.P., Wu, W., Liu, H.B., 2013. General models for estimating daily global solar radiation for different solar radiation zones in mainland China. Energ. Conver. Manage. 70, 139–148.

Lionetto, M.G., Guascito, M.R., Giordano, M.E., Caricato, R., De Bartolomeo, A.R., Romano, M.P., et al., 2021. Oxidative potential, cytotoxicity, and intracellular oxidative stress generating capacity of PM10: a case study in south of Italy. Atmosphere 12 (4), 464.

Liu, Q., Baumgartner, J., Zhang, Y., Liu, Y., Sun, Y., Zhang, M., 2014. Oxidative potential and inflammatory impacts of source apportioned ambient air pollution in Beijing. Environ. Sci. Technol. 2014 (48), 12920–12929.

Manousakas, M., Furger, M., Daellenbach, K.R., Canonaco, F., Chen, G., Tobler, A., Rai, P., Qi, L., Tremper, A.H., Green, D., Hueglin, C., Slowik, J.G., El Haddad, I., Prevot, A.S.H., 2022. Source identification of the elemental fraction of particulate matter using size segregated, highly time-resolved data and an optimized source apportionment approach. Atmos. Environ. X 14, 100165.

Marenco, F., Bonasoni, P., Calzolari, F., Ceriani, M., Chiari, M., Cristofanelli, P., D'Alessandro, A., Fermo, P., Lucarelli, F., Mazzei, F., Nava, S., Piazzalunga, A., Prati, P., Valli, G., Vecchi, R., 2006. Characterization of atmospheric aerosols at Monte Cimone, Italy, during summer 2004: source apportionment and transport mechanism. J. Geophys. Res. 111, D24202.

Massimi, L., Ristorini, M., Astolfi, M.L., Perrino, C., Canepari, S., 2020. High resolution spatial mapping of element concentrations in PM10: a powerful tool for localization of emission sources. Atmos. Res. 244, 105060.

Massimi, L., Wesseling, J., van Ratingen, S., Javed, I., Frezzini, M.A., Astolfi, M.L., Canepari, S., Vermeulen, R., 2021. Identification and spatial mapping of tracers of PM10 emission sources using a high spatial resolution distributed network in an urban setting. Atmos. Res. 262, 105771.

Massimi, L., Frezzini, M.A., Amoroso, A., Di Giosa, A.D., Martino, L., Tiraboschi, C., Messi, M., Astolfi, M.L., Perrino, C., Canepari, S., 2024. Spatially resolved chemical data for PM10 and oxidative potential source apportionment in urban-industrial settings. Urban Clim. 58, 102113.

Merico, E., Cesari, D., Dinoi, A., Gambaro, A., Barbaro, E., Guascito, M.R., Giannossa, L. C., Mangone, A., Contini, D., 2019. Inter-comparison of carbon content in PM10 and PM2.5 measured with two thermo-optical protocols on samples collected in a Mediterranean site. Environ. Sci. Pollut. Res. 26, 29334–29350.

Molina, C., Toro, A.R., Manzano, C.A., Canepari, S., Massimi, L., Leiva-Guzman, M., 2020. Airborne aerosols and human health: leapfrogging from mass concentration to oxidative potential. Atmosphere 11 (9), 917.

Ostro, B., Malig, B., Hasheminassab, S., Berger, K., Chang, E., Sioutas, C., 2016. Associations of source-specific fine particulate matter with emergency department visits in California. Am. J. Epidemiol. 184, 450–459.

Øvrevik, J., 2019. Oxidative potential versus biological effects: a review on the relevance of cell-free/abiotic assays as predictors of toxicity from airborne particulate matter. Int. J. Mol. Sci. 20, 4772.

Paatero, P., Hopke, P.K., 2003. Discarding or down weighting high-noise variables in factor analytic models. Anal. Chim. Acta 490, 277–289.

Paatero, P., Eberly, S., Brown, S.G., Norris, G.A., 2014. Methods for estimating uncertainty in factor analytic solutions. Atmos. Meas. Tech. 7 (3), 781–797.

Paraskevopoulou, D., Bougiatioti, A., Stavroulas, I., Fang, T., Lianou, M., Liakakou, E., Gerasopoulos, E., Weber, R., Nenes, A., Mihalopoulos, N., 2019. Yearlong variability of oxidative potential of particulate matter in an urban Mediterranean environment. Atmos. Environ. 206, 183–196.

Perrino, C., Catrambone, M., Dalla Torre, S., Rantica, E., Sargolini, T., Canepari, S., 2014. Seasonal variations in the chemical composition of particulate matter: a case study in the Po Valley. Part I: macro-components and mass closure. Environ. Sci. Pollut. Res. 21, 3999–4009.

Perrone, M.R., Bertoli, I., Romano, S., Russo, M., Rispoli, G., Pietrogrande, M.C., 2019. PM2.5 and PM10 oxidative potential at a Central Mediterranean Site: Contrasts between dithiothreitol-and ascorbic acid-measured values in relation with particle size and ascorbic acid-measured values in relation with particle size and chemical composition. Atmos. Environ. 210, 143–155.

Pey, J., P'erez, N., Castillo, S., Viana, M., Moreno, T., Pandolfi, M., et al., 2009. Geochemistry of regional background aerosols in the Western Mediterranean. Atmos. Res. 94, 422–435.

Pietrodangelo, A., Bove, M.C., Forello, A.C., Crova, F., Bigi, A., Brattich, E., Riccio, A., Becagli, S., Bertinetti, S., Calzolai, G., Canepari, S., Cappelletti, D., Catrambone, M., Cesari, D., Colombi, C., Contini, D., Cuccia, E., De Gennaro, G., Genga, A., Ielpo, P., Lucarelli, F., Malandrino, M., Masiol, M., Massabò, D., Perrino, C., Prati, P., Siciliano, T., Tositti, L., Venturini, E., Vecchi, R., 2024. A PM10 chemically characterized nation-wide dataset for Italy. Geographical influence on urban air pollution and source apportionment. Sci. Total Environ. 908, 167891.

Pietrogrande, M.C., Demaria, G., Colombi, C., Cuccia, E., Dal Santo, U, 2022. Seasonal and Spatial Variations of PM_{10} and $PM_{2.5}$ Oxidative Potential in Five Urban and Rural Sites across Lombardia Region, Italy. Int. J. Environ. Res. Public Health 19 (13), 7778.

Querol, X., Alastuey, A., Moreno, T., Viana, M.M., Castillo, S., Pey, J., et al., 2008. Spatial and temporal variations in airborne particulate matter (PM10 and PM2.5) across Spain 1999–2005. Atmos. Environ. 42, 3964–3979.

Rivas, I., Vicens, L., Basagaña, X., Tobías, A., Katsouyanni, K., Walton, H., et al., 2021. Associations between sources of particle number and mortality in four European cities. Environ. Int. 155, 106662.

Rönkkö, T.J., Hirvonen, M.-R., Happo, M.S., Ihantola, T., Hakkarainen, H., Martikainen, M.-V., Gu, C., Wang, Q.G., Jokiniemi, J., Komppula, M., Jalava, P.I., 2021. Inflammatory responses of urban air PM modulated by chemical composition and different air quality situations in Nanjing, China. Environ. Res. 192, 110382.

Salameh, D., Detournay, A., Pey, J., Pérez, N., Liguori, F., Saraga, D., Bove, M.C., Brotto, P., Cassola, F., Massabò, D., Latella, A., Pillon, S., Formenton, G., Patti, S., Armengaud, A., Piga, D., Jaffrezo, J.L., Bartzis, J., Tolis, E., Prati, P., Querol, X., Wortham, H., Marchand, N., 2015. PM2.5 chemical composition in five European Mediterranean cities: a 1-year study. Atmos. Res. 155, 102–117.

Sandrini, S., Fuzzi, S., Piazzalunga, A., Prati, P., Bonasoni, P., Cavalli, F., Bove, M.C., Calvello, M., Cappelletti, D., Colombi, C., Contini, D., de Gennaro, G., Di Gilio, A., Fermo, P., Ferrero, L., Gianelle, V., Giugliano, M., Ielpo, P., Lonati, G., Marinoni, A., Massabò, D., Molteni, U., Moroni, B., Pavese, G., Perrino, C., Perrone, M.G., Perrone, M.R., Putaud, J.P., Sargolini, T., Vecchi, R., Gilardoni, S., 2014. Spatial and seasonal variability of carbonaceous aerosol across Italy. Atmos. Environ. 99, 587–598.

Szidat, S., Jenk, T.M., Synal, H.A., Kalberer, M., Wacker, L., Hajdas, I., Kasper-Giebl, A., Baltensperger, U., 2006. Contributions of fossil fuel, biomass-burning, and biogenic emissions to carbonaceous aerosols in Zurich as traced by 14C. J. Geophys. Res. 111, D07206.

in't Veld, M., Pandolfi, M., Amato, F., Pérez, N., Reche, C., Dominutti, P., Jaffrezo, J., Alastuey, A., Querol, X., Uzu, G., 2023. Discovering oxidative potential (OP) drivers of atmospheric PM10, PM2.5, and PM1 simultaneously in north-eastern Spain. Sci. Total Environ. 857, 159386.

Tositti, L., Brattich, E., Masiol, M., Baldacci, D., Ceccato, D., Parmeggiani, S., Stracquadanio, M., Zippoli, S., 2014. Source apportionment of particulate matter in a large city of southeastern Po valley (Bologna, Italy). Environ. Sci. Pollut. Res. 21, 872–890.

Watson, J.G., Zhu, T., Chow, J.C., Engelbrecht, J., Fujita, E.M., Wilson, W.E., 2002. Receptor modelling application framework for particle source apportionment. Chemosphere 49, 1093–1136.

Weber, S., Uzu, G., Favez, O., Borlaza, L.J.S., Calas, A., Salameh, D., Chevrier, F., Allard, J., Besombes, J.-L., Albinet, A., Pontet, S., Mesbah, B., Gille, G., Zhang, S., Pallares, C., Leoz-Garziandia, E., Jaffrezo, J.-L., 2021. Source apportionment of atmospheric PM_{10} oxidative potential: synthesis of 15 year-round urban datasets in France. Atmos. Chem. Phys. 21, 11353–11378.

Zhang, R., Han, Z., Shen, Z., Cao, J., 2008. Continuous measurement of number concentrations and elemental composition of aerosol particles for a dust storm event in Beijing. Adv. Atmos. Sci. 25, 89–95.

Zhang, Z., Sun, Y., Chen, C., You, B., Du, A., Xu, W., Li, Y., Li, Z., Lei, L., Zhou, W., Sun, J., Qiu, Y., Wei, L., Fu, P., Wang, Z., 2022. Sources and processes of water-soluble and water-insoluble organic aerosol in cold season in Beijing, China. Atmos. Chem. Phys. 22, 10409–10423.